A Pro-Chelator Triggered by Hydrogen Peroxide Inhibits Iron-Promoted Hydroxyl Radical Formation

ARTICLE *in* JOURNAL OF THE AMERICAN CHEMICAL SOCIETY · OCTOBER 2006

Impact Factor: 12.11 · DOI: 10.1021/ja064806w · Source: PubMed

3 AUTHORS, INCLUDING:

Katherine J Franz
Duke University
57 PUBLICATIONS **1,524** CITATIONS

SEE PROFILE

J|A|C|S
COMMUNICATIONS

Published on Web 09/01/2006

A Pro-Chelator Triggered by Hydrogen Peroxide Inhibits Iron-Promoted Hydroxyl Radical Formation

Louise K. Charkoudian, David M. Pham, and Katherine J. Franz*

Department of Chemistry, Duke University, P.O. Box 90346, Durham, North Carolina 27708

Received July 6, 2006; E-mail: katherine.franz@duke.edu

Neurodegenerative diseases such as Parkinson's and Alzheimer's diseases show signs of increased oxidative stress that result when reactive oxygen species (ROS) overwhelm a cell's inherent antioxidant mechanisms.[1−4] Markers of oxidative stress include lipid peroxidation, DNA base hydroxylation, and protein modification, all of which are attributed to the highly reactive hydroxyl radical, $OH^{\bullet}$. While many potential antioxidant therapies use radical scavengers in attempts to mitigate cellular damage, such strategies do not inhibit formation of these harmful radicals.

A principal mechanism for the formation of $OH^{\bullet}$ is via iron-promoted reactions like the Fenton reaction (eq 1),[5] which becomes catalytic if cellular reductants can reduce Fe^{3+} to Fe^{2+}.

$$Fe^{2+} + H_2O_2 \rightarrow Fe^{3+} + OH^{\bullet} + OH^{-} \qquad (1)$$

In order for iron to promote Fenton chemistry, it must be in a coordination environment that favors redox cycling and allows reactants access to the inner sphere of the metal center.[6] These requirements imply that loosely bound iron that is not properly regulated by the cell's normal metal trafficking and storage mechanisms contributes to oxidative stress.[1,2,4] Chelating agents that can selectively sequester this pool of iron could potentially inhibit iron-promoted oxidative stress by inactivating the source itself. Although several chelators that were developed to treat iron overload diseases have some desirable properties for treating neurodegenerative diseases,[7−10] they also have troubling drawbacks.[11] Their high affinity for iron means that they compete with iron-binding proteins, thereby altering healthy iron distribution and inhibiting essential iron-containing enzymes. Furthermore, their intrinsic affinity for other metal ions disrupts the availability of key elements like zinc.

To overcome these limitations, we are developing a class of pro-chelators that have little to no affinity for metal ions until a protective mask is selectively removed by ROS, as demonstrated in Scheme 1 for H_2O_2. In the absence of oxidative stress, these masked molecules are poor ligands that cannot alter healthy metal ion distribution, a common toxicity issue associated with currently available chelation therapies. Disease conditions that elevate oxidative stress, however, activate the chelator to reveal a high-affinity ligand that scavenges and incapacitates redox-active iron that is the source of $OH^{\bullet}$ generation.

Herein we present our first-generation pro-chelator, **BSIH**, in which a boronic ester conceals a latent phenolic oxygen that is a key donor atom of salicylaldehyde isonicotinoyl hydrazone (**SIH**), a member of the well-known aroylhydrazone class of chelators that show considerable promise as orally available agents.[12−14]

Aryl boronic esters react selectively with H_2O_2 to produce phenols,[15,16] which are excellent metal-binding groups often incorporated into multidentate ligands. Boronate-based fluoresceins have been used as intracellular fluorescence probes of H_2O_2, work that demonstrates the selectivity and biocompatibility of this class of molecules.[15,16]

Scheme 1

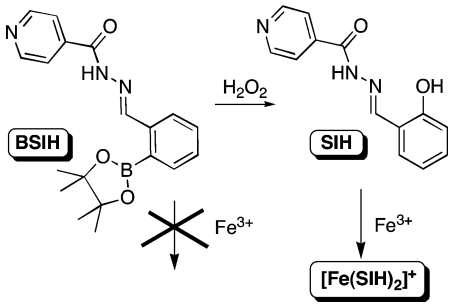

The pro-chelate **BSIH** is readily obtained by condensation of isonicotinic acid hydrazide with (2-formylphenyl)boronic acid pinacol ester (**Bsal**). The X-ray structure in Figure 1 reveals an *E* configuration about the C7═N3 double bond and an anti configuration of the B atom with respect to the imine N3 atom. NMR reveals that other conformations are accessible in solution (Supporting Information). Reaction with H_2O_2 converts **BSIH** cleanly to **SIH**, as confirmed by NMR. The OH group of **SIH** adopts a syn conformation that is favorably disposed for tridentate metal chelation via the carbonyl O, the imine N, and the deprotonated phenolate O^-.[17]

As shown in Figure 2, addition of Fe^{3+} to a solution of **BSIH** introduces a shoulder in the UV−vis spectrum at 380 nm which is attributed to $Fe(NO_3)_3$ and a slight decrease at 300 nm which may indicate a weak interaction. The absence of new features suggests that a tight Fe^{3+} complex does not form. The addition of H_2O_2 to this mixture, however, results in a new spectrum matching that of $[Fe(\mathbf{SIH})_2]^+$, or $[Fe(\mathbf{SIH})]^{2+}$ at low ligand/metal ratios. These two species, which form immediately upon mixing, are distinguishable by a ligand-field band at 658 nm that is more pronounced in the mono species than the bis (Figure 2 inset).

Figure 3 shows the time course for iron complex formation following addition of excess H_2O_2 to a methanol solution of $Fe(NO_3)_3$ and **BSIH**. Although the kinetics are complicated by the mono to bis $Fe(\mathbf{SIH})_x$ coordination, the data fit a pseudo-first-order

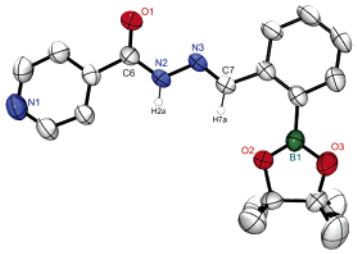

Figure 1. ORTEP diagram of **BSIH** showing 50% thermal ellipsoids. Selected bond distances: C6−O1, 1.228(3); N2−N3, 1.384(2); N3−C7, 1.276(3) Å.

10.1021/ja064806w CCC: $33.50

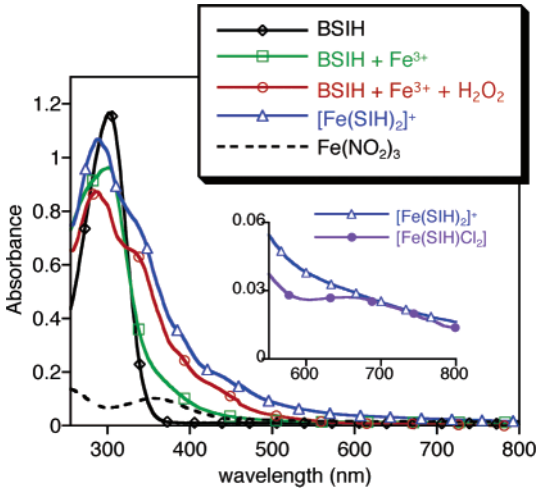

Figure 2. UV−vis spectra of 60 μM **BSIH** in MeOH in the absence and presence of 30 μM $Fe(NO_3)_3$. Addition of 0.6 mM H_2O_2 results in a spectrum (open red circles) matching that of $[Fe(\mathbf{SIH})_2]^+$ (blue triangles). The expanded view in the inset compares the mono and bis species, $[Fe(\mathbf{SIH})Cl_2(CH_3OH)]$ and $[Fe(\mathbf{SIH})_2]NO_3$, respectively, at 60 μM.

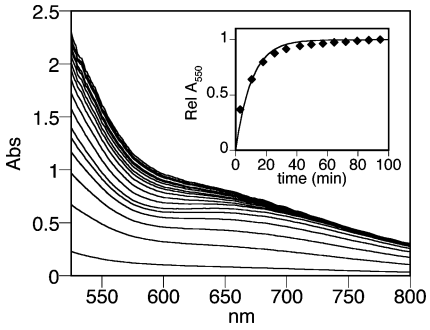

Figure 3. UV−vis spectra showing the formation of $[Fe(\mathbf{SIH})]^{2+}$ and $[Fe(\mathbf{SIH})_2]^+$ upon addition of 100 mM H_2O_2 to a solution of 1.5 mM $Fe(NO_3)_3$ and 3.0 mM **BSIH** in MeOH.

expression to give $k_{obs} = 1.6 \times 10^{-3}$ s^{-1}. This value is consistent with preliminary kinetic data for the conversion of **BSIH** to **SIH** in the absence of iron (not shown), indicating that the rate-limiting step for iron sequestration is oxidation of **BSIH** to **SIH**, followed by rapid metal complexation.

To test the effectiveness of **BSIH** for inhibiting OH$^\bullet$ formation, we used an in vitro deoxyribose assay in which hydroxyl radicals that are generated via typical Fenton conditions of Fe^{3+}, ascorbic acid, and H_2O_2 degrade deoxyribose to give products that form a chromophore with thiobarbituric acid (TBA) with λ_{max} at 532 nm.[18] Figure 4 displays the effect of increasing chelator concentration on the degradation of deoxyribose under these conditions. Values of A/A_o above 1 indicate that the additive promotes OH$^\bullet$ formation, whereas values below 1 indicate that the additive either scavenges OH$^\bullet$ more efficiently than deoxyribose, or that it inhibits iron-catalyzed OH$^\bullet$ formation via effective iron chelation. EDTA, a ligand known to promote Fenton chemistry, causes a significant increase in A/A_o (Supporting Information), whereas desferrioxamine (**DFO**) and **SIH**, chelators known to inhibit Fenton chemistry,[19] show a decrease in A/A_o. As shown in Figure 4, **BSIH** protects against deoxyribose degradation as well as both **DFO** and **SIH**.

To show that the protective effect of **BSIH** is not solely due to consumption of H_2O_2, we tested the boronate-masked salicylaldehyde, **Bsal**, which converts to salicylaldehyde (**Sal**) in the presence of H_2O_2. Neither **Bsal** nor **Sal** has a significant influence on the

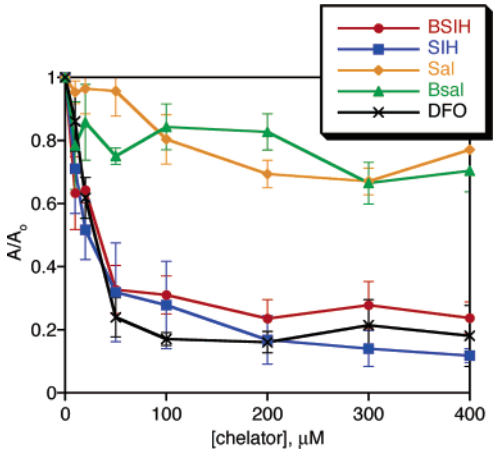

Figure 4. Effect of chelator concentration on deoxyribose degradation by OH$^\bullet$. A and A_o are the absorbance at 532 nm in the presence and absence of chelator, respectively. Values below $A/A_o = 1$ indicate protection of deoxyribose. Conditions: 200 μM H_2O_2, 10 μM $FeCl_3$, 2 mM ascorbic acid, 15 mM deoxyribose in pH 7.4 $NaHPO_4$ buffer.

deoxyribose assay, as shown by the nearly constant A/A_o values near unity in Figure 4. Whereas **DFO** and **SIH** protect deoxyribose when OH$^\bullet$ are generated in the absence of added H_2O_2, **BSIH** has little effect under these conditions (Supporting Information). Taken together, these data indicate that the protective effect of **BSIH** against deoxyribose degradation derives from its H_2O_2-dependent conversion to **SIH**, which in turn provides the right coordination environment around Fe to prevent iron-promoted OH$^\bullet$ generation.

Acknowledgment. We thank Duke University and the Parkinson's Disease Foundation for support.

Supporting Information Available: Complete refs 9 and 10, experimental details, and X-ray crystallographic data, including CIF files. This material is available free of charge via the Internet at http://pubs.acs.org.

References

(1) Barnham, K. J.; Masters, C. L.; Bush, A. I. *Nat. Rev. Drug Discov.* **2004,** *3*, 205−214.
(2) Jellinger, K. A. *Drugs Aging* **1999,** *14*, 115−140.
(3) Shults, C. W. *Antioxid. Redox Signaling* **2005**, *7*, 694−700.
(4) Zecca, L.; Youdim, M. B. H.; Riederer, P.; Conner, J. R.; Crichton, R. R. *Nat. Rev. Neurosci.* **2004**, *5*, 863−873.
(5) Dunford, H. B. *Coord. Chem. Rev.* **2002**, *233*, 311−318.
(6) Liu, Z. D.; Hider, R. C. *Coord. Chem. Rev.* **2002**, *232*, 151−171.
(7) Richardson, D. R. *Ann. N.Y. Acad. Sci.* **2004**, *1012*, 326−341.
(8) Youdim, M. B. H.; Stephenson, G.; Ben Shachar, D. *Ann. N.Y. Acad. Sci.* **2004**, *1012*, 306−325.
(9) Kaur, D.; et al. *Neuron* **2003**, *37*, 899−909.
(10) Ritchie, C. W.; et al. *Arch. Neurol.* **2003**, *60*, 1685−1691.
(11) Benvenisti-Zarom, L.; Chen, J.; Regan, R. F. *Neuropharmacology* **2005**, *49*, 687−694.
(12) Kalinowski, D. S.; Richardson, D. R. *Pharmacol. Rev.* **2005**, *57*, 547−583.
(13) Horackova, M.; Ponka, P.; Byczko, Z. *Cardiovasc. Res.* **2000**, *47*, 529−536.
(14) Simunek, T.; Boer, C.; Bouwman, R. A.; Vlasblom, R.; Versteilen, A. M. G.; Sterba, M.; Gersl, V.; Hrdina, R.; Ponka, P.; de Lange, J. J.; Paulus, W. J.; Musters, R. J. P. *J. Mol. Cell. Cardiol.* **2005**, *39*, 345−354.
(15) Chang, M. C. Y.; Pralle, A.; Isacoff, E. Y.; Chang, C. J. *J. Am. Chem. Soc.* **2004**, *126*, 15392−15393.
(16) Miller, E. W.; Albers, A. E.; Pralle, A.; Isacoff, E. Y.; Chang, C. J. *J. Am. Chem. Soc.* **2005**, *127*, 16652−16659.
(17) Yin, H. D.; Hong, M.; Li, G.; Wang, D. Q. *J. Organomet. Chem.* **2005**, *690*, 3714−3719.
(18) Halliwell, B.; Gutteridge, J. M. C.; Aruoma, O. I. *Anal. Biochem.* **1987**, *165*, 215−219.
(19) Hermes-Lima, M.; Ponka, P.; Schulman, H. M. *Biochim. Biophys. Acta* **2000**, *1523*, 154−160.

JA064806W